ISSN 1560-0904, Polymer Science, Series B, 2020, Vol. 62, No. 6, pp. 750–755. © Pleiades Publishing, Ltd., 2020.

COMPOSITES

Synthesis and Characterization of Hybrid Material Based on Poly(pyrrole-*co*-*N*-methyl pyrrole) and $ZnCo_2O_4$

Boualem Alouche[a], Ahmed Yahiaoui[a], and Abdelkader Dehbi[b,*]

[a] *Laboratoire de Chimie Organique, Macromoléculaire et des Matériaux, Faculté des Sciences Exactes, University of Mascara, 29000 Algérie*

[b] *Engineering Physics Laboratory, Universiy of Tiaret, Tiaret, 14000 Algérie*

**e-mail: abddehbi@gmail.com*

Received July 6, 2020; revised September 8, 2020; accepted October 8, 2020

Abstract—This study highlights the method of synthesis and characterization of a novel hybrid material consisting of zinc cobaltite ($ZnCo_2O_4$) and the conductive copolymer based on pyrrole and *N*-methyl pyrrole. The pure $ZnCo_2O_4$ is synthesized by sol-gel method, polypyrrole-$ZnCo_2O_4$, poly(*N*-methyl pyrrole)-$ZnCo_2O_4$ and poly(pyrrole-*co*-*N*-methyl pyrrole)-$ZnCo_2O_4$ are synthesized by chemical oxidative polymerization and characterized by different techniques. X-ray diffraction results revealed the existence of a cubic spinel structure of $ZnCo_2O_4$ in all samples. The synthesis efficiency of the polymer-$ZnCo_2O_4$ nanocomposite is confirmed by the Fourier transform infrared spectroscopy. The results of scanning electron microscopy show that the nanoparticles are mostly spherical in shape and the powders morphology structure varies from sample to sample. The energy dispersive X-ray analysis shows the formation of hybrid material with a substantial purity.

DOI: 10.1134/S1560090420330015

INTRODUCTION

Hybrid organic-inorganic materials containing inorganic and organic components are of a great interest due to their characteristics, resulting in synergistic improvement of their functional properties [1, 2].

In recent years, conductive polymers have attracted considerable interest for the development of advanced materials; the advantage of these polymers is their processability, especially through the solution process [3]. Conductive polymers, such as polypyrrole (PPy), have been proposed for various applications, e.g. solar cells [4], transistors [5], thermoelectric power-generation [6], microwave absorption [7], electrochromic devices [8], photocurrent generation [9], supercapacitors [10] and light emitting diodes [11, 12]. However cycling instability and rate capability restrict practical applications of conductive polymer. Recently, much efforts have been focused on the development of hybrid nanomaterials based on PPy, such as metal-polypyrrole core-shell nanoparticles and metal-polypyrrole hybrid nanowires, in order to improve the polymer stability [13]. In these hybrid materials, metal nanoparticles function as a skeleton for docking electroactive materials that can hold the electrode fragments together, and improve the stability of PPy. Particularly, $ZnCo_2O_4$ exhibits a higher stability than that of PPy materials [14].

Spinel is oxide of formulas AB_2O_4, where A and B are generally elements belonging to transition metals; Table 1 summarizes the difference between three materials of the same spinel family AB_2O_4. The typical representative of the spinel is $ZnCo_2O_4$. For the $ZnCo_2O_4$ system a cubic face arrangement centered anions O^{2-} is described. The space group of the crystalline is Fd3m. From a structural point of view, the elementary cell of the general formula "$A_8B_{16}O_{32}$", contains 32 O^{2-} anions that delineate 64 tetrahedral sites (rated A) and 32 sites octahedral (rated B) occupied respectively by the eighth and half cations and which corresponds to 8 units forms AB_2O_4 per elemental cell. The inorganic phase is the metal oxide part that has attracted significant scientific interest, such as the spinel zinc cobaltite ($ZnCo_2O_4$) is isomorphic to the Co_3O_4 crystal structure and seems to be a promising alternative, due to its higher conductivity and richer redox reactions, caused by the coupling of the two metal species [15].

The $ZnCo_2O_4$, a ternary oxide material, has been reported as a promising electrode material for lithium-ion batteries. With a cubic spinel structure, $ZnCo_2O_4$ is isomorphic to Co_3O_4, i.e., Zn^{2+} ions occupy the tetrahedral sites and the Co^{3+} ions occupy the octahedral sites, revealing superior electroactivity to Co_3O_4. In addition, Zn element has many other advantages,

Table 1. Electrical properties of pure $ZnCo_2O_4$, $ZnRh_2O_4$, and $NiCo_2O_4$

Samples	Specific capacitance, F/g	Electrical conductivity, S/cm	Gap energy, eV
$ZnCo_2O_4$	290 [42]	1.8 [44]	2.26 [45]
$ZnRh_2O_4$	950 [43]	0.7 [46]	2.74 [46]
$NiCo_2O_4$	1580 [17]	0.12 [47]	3.3 [48]

including low cost, abundant resources and environment friendliness. It is well known that the large volume change associated with lithiation–delithiation of TMOs is a very common phenomenon, which can significantly impede the practical application of TMO-based anodes [16, 17].

Among the p-type semiconductors, zinc cobaltite ($ZnCo_2O_4$) is a material with spinel-type structure that has been mainly used as electrode for Li-ion batteries [18, 19] and supercapacitors [20, 21], due to its higher electrochemical performances and super conductivities.

Nirav Joshi et al. [22] have shown that $ZnCo_2O_4$ microspheres can be synthesized by co-precipitation and subsequent annealing. The yolk-shelled $ZnCo_2O_4$ sensor was highly sensitive to detect ozone down to 80 ppb with both a.c. and d.c. electrical measurements, with fast response and recovery, and good selectivity. The mechanism of detection was found to be based on adsorption of ozone molecules on the $ZnCo_2O_4$ surface, as a layer of holes is created which affects the conductivity, as in a typical *p*-type semiconductor. Finally, the enhanced performance owing to the large surface area to volume ratio of $ZnCo_2O_4$ yolk-shelled microspheres are promising for developing further gas sensor devices to monitor the environment [23].

In this research, pyrrole and *N*-methyl pyrrole are used. The process of synthesis and characterization of hybrid material poly(Py-*co*-NMPy)-$ZnCo_2O_4$ nanocomposites by in situ polymerization method is emphasized. The properties of nanocomposites, morphology, thermal stability and electrical conductivity have been investigated.

EXPERIMENTAL

Materials

Pyrrole, *N*-methylpyrrole, ammonium persulfate ($(NH_4)_2S_2O_8$, 98%), hydrochloric acid (36.5–38.0%), ethanol (99.7% purity) and ammonium hydroxide are obtained from Aldrich. Distilled water is obtained from Elga Labwater Purelab Ultra system.

Preparation of $ZnCo_2O_4$

The zinc cobaltite ($ZnCo_2O_4$) solution is obtained by sol-gel method by dissolving of 2.11 g of a tetrahydrated zinc nitrate powder ($Zn(NO_3)_2 \cdot 4H_2O$) in 20 mL of ethanol. The mixture is stirred or 10 min until the colorless solution is obtained. Then 4.70 g of hexahydrated cobalt nitrates ($Co(NO_3)_2 \cdot 6H_2O$) is dissolved in 30 mL of ethanol to produce dark purple solution. After that two solutions are mixed and a solution of oxalic acid prepared by dissolving 7 mg of $C_2H_2O_4$ in 50 mL of ethanol is added. The overall mixture is slowly heated to 80°C for 2 h with magnetic stirring. The $ZnCo_2O_4$ solution is dried at 120°C for 12 h and then charred at 350°C for 2 h to obtain a well-crystallized black powder [24].

Preparation of Nanocomposites

The hybrid material is prepared by the oxidative polymerization. Thus, 0.5 g of $ZnCo_2O_4$ nanopowder functionalized by 1 M HCl is added to 0.05 mol of pyrrole and/or *N*-methyl pyrrole solution in 50 mL of HCl 0.1 M and stirred for 1 h. Then, an aqueous solution of APS (0.05 mol) is added drop wise and the mixture is stirred for 24 h, while the temperature is maintained at 0–5°C by an ice bath.

The precipitated nanocomposite is filtered and washed with ethanol until the filtrate become colorless, then with water for three times and finally, with NH_4OH. The precipitates are dried at 60°C for 24 h to obtain a black dark powder.

Three different samples of polymer-$ZnCo_2O_4$ nanocomposites are synthesized, polypyrrole-$ZnCo_2O_4$, poly(*N*-methyl pyrrole)-$ZnCo_2O_4$ and poly(pyrrole-*co*-*N*-methyl pyrrole)-$ZnCo_2O_4$ [25, 26].

RESULTS AND DISCUSSION

The crystalline phases of the samples are identified by using a diffractometer with CuK_α radiation (λ = 1.5406 Å) and a scan speed of 5 grad/min. The resulting spectrum is identified by comparison with the corresponding JCPD.

All the lines observed on the diffractograms (Fig. 1) correspond to the planes (111), (220), (311), (222), (400), (422), (511) and (440) and can be attributed to the cubic spinel structure of $ZnCo_2O_4$ (JCPDS no. 23-1390, characteristic of space group Fd_3m and a mesh parameter a = 8.0717 Å) [27], with preferential orientation according to (311). Table 2 shows that the diffraction nail, interreticular distance and lattice parameter of all planes structure of $ZnCo_2O_4$.

X-ray diffraction spectra are used to determine the particle size of the nanoparticles. The particle size is

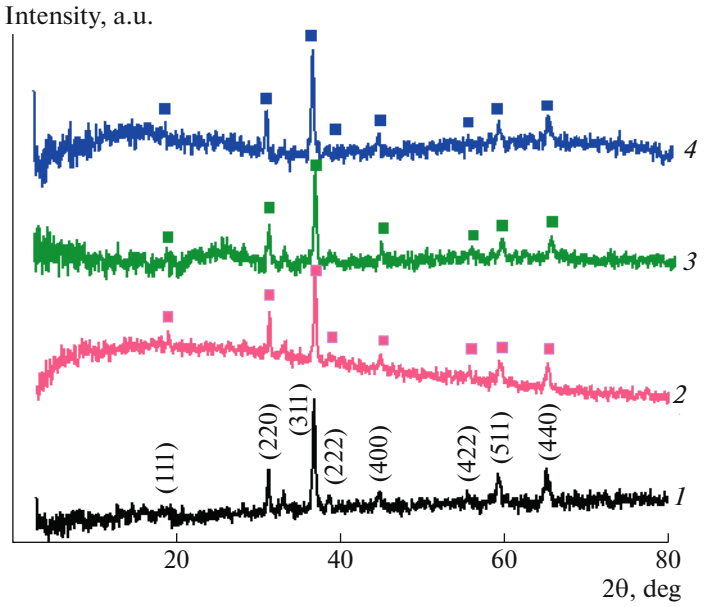

Fig. 1. XRD diffraction patterns of (*1*) $ZnCo_2O_4$, (*2*) poly(NMPy)-$ZnCo_2O_4$, (*3*) PPy-$ZnCo_2O_4$, and (*4*) poly(Py-*co*-NMPy)-$ZnCo_2O_4$ nanocomposites.

calculated by using the formula of Debye-Scherrer [28] applied to the diffraction line (311):

$$D = \frac{0.9\lambda}{\beta\cos\theta},$$

$$\beta = \frac{0.30 \times 3.14}{180} = 0.005233 \text{ rad},$$

$$D = \frac{0.9 \times 1.5406}{0.005233 * \cos(18.4540)},$$

$$D = 279.3242 \text{ Å}.$$

FTIR spectra of samples $ZnCo_2O_4$, PPy-$ZnCo_2O_4$, PNMPy-$ZnCo_2O_4$ and poly(Py-*co*-NMPy)-$ZnCo_2O_4$, clearly show the existence of characteristic bands of polymer and zinc cobaltite (Fig. 2). For nanoparticles of $ZnCo_2O_4$, the adsorption bands at 663 and 527 cm^{-1} are attributed to the tetrahedral and octahedral coordination vibrations of Zn–O and Co–O respectively [29]. The band at 1635 cm^{-1} can be assigned to the vibrations of –OH groups for free or absorbed water [30].

For the hybrid materials PPy-$ZnCo_2O_4$, PNMPy-$ZnCo_2O_4$ and P(Py-*co*-NMPy)-$ZnCo_2O_4$, the existence of wide bands with low intensity at 3227 cm^{-1} is attributed to the stretch vibration N–H of the pyrrole [31] and the bands 2970 and 2875 cm^{-1} are related to the groups stretching CH_3 of PNMPy [32, 33]. The bands at 1600–1540 cm^{-1} arise from C=C stretching vibrations of the aromatic rings [34, 35], the bands observed at 1519 and 1444 cm^{-1} are attributed to the asymmetric and symmetric ring stretching vibrations of the pyrrole respectively [36–38]. The C–N stretching vibrations are observed at 1272 cm^{-1}. The bands between 1025 and 909 cm^{-1} can be attributed to C–H in plane and C–H out of plane deformations respectively [39, 40].

Table 2. Structural characteristics of $ZnCo_2O_4$

Miller indices (*hkl*)	Diffraction nail θ, deg	Interreticular distance d_{hkl}, Å	Lattice parameter *a*, Å
(111)	9.53	4.65	8.06
(220)	15.60	2.86	8.10
(311)	18.45	2.43	8.07
(222)	19.40	2.32	8.03
(400)	22.51	2.01	8.05
(511)	29.68	1.56	8.08
(440)	32.51	1.43	8.11

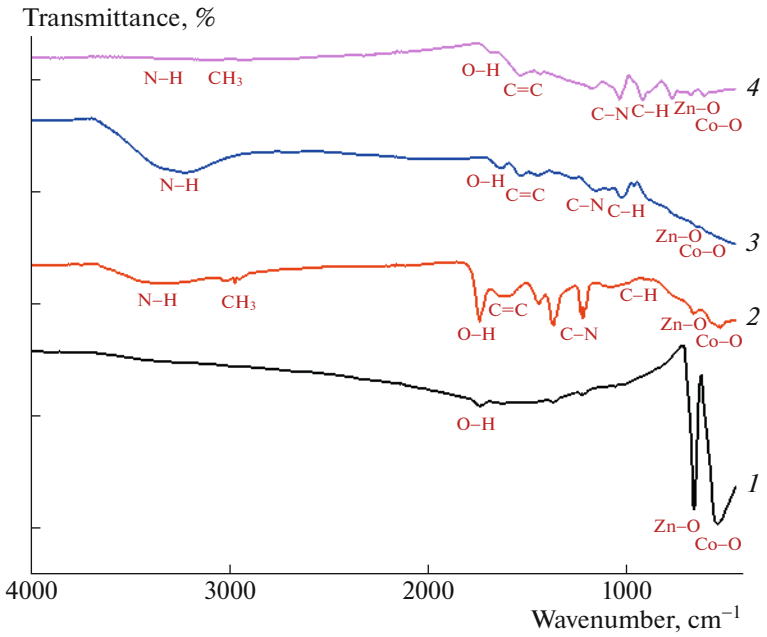

Fig. 2. FTIR spectra of the (*1*) $ZnCo_2O_4$, (*2*) poly(*N*-methyl pyrrole)-$ZnCo_2O_4$, (*3*) polypyrrole-$ZnCo_2O_4$, and (*4*) poly(pyrrole-*co*-*N*-methyl pyrrole)-$ZnCo_2O_4$.

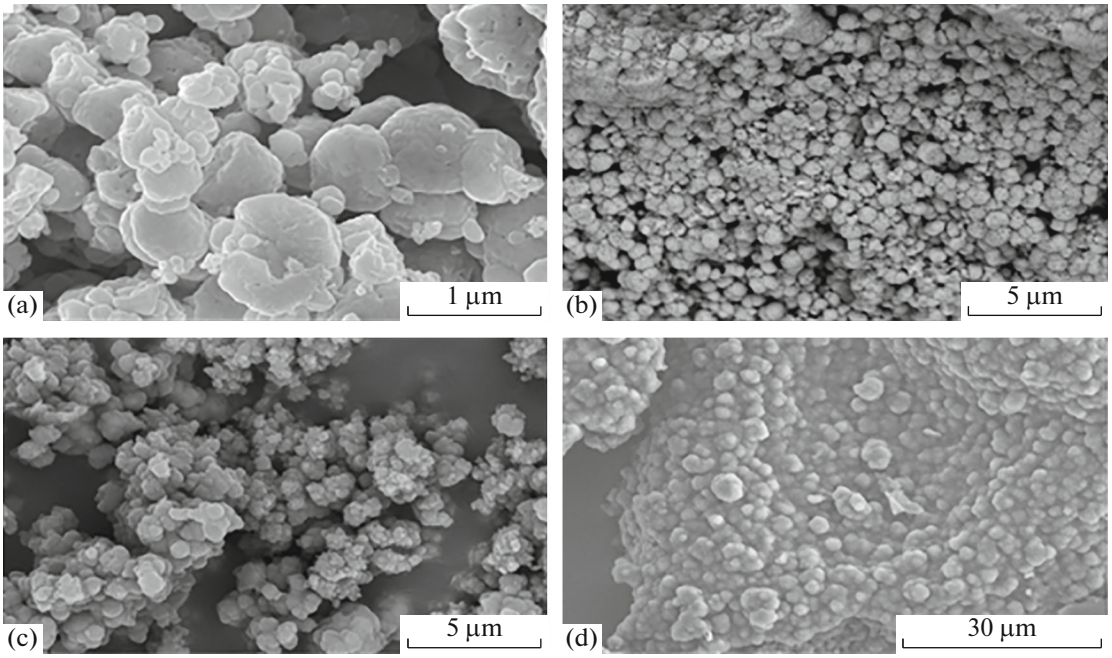

Fig. 3. The SEM images of (a) $ZnCo_2O_4$, (b) PNMPy-$ZnCo_2O_4$, (c) PPy-$ZnCo_2O_4$, and (d) P(Py-co-NMPy)-$ZnCo_2O_4$ nanocomposites.

Figure 3 shows the SEM micrographs of $ZnCo_2O_4$ and nanocomposites. All micrographs reveal a complete encapsulation of $ZnCo_2O_4$ in the polymer matrix. The overall particles are spherical in shape with an irregular size distribution throughout, this is due to the formation of many agglomerates, the particles in the samples are in the nanoscale range, which confirms the results obtained by XRD.

The EDX spectrum shown in the Fig. 4 shows the presence of the five constituent elements of the synthesized material, namely, C, N, Co, Zn, and O, indicating the formation of $ZnCo_2O_4$ and poly(Py-*co*-

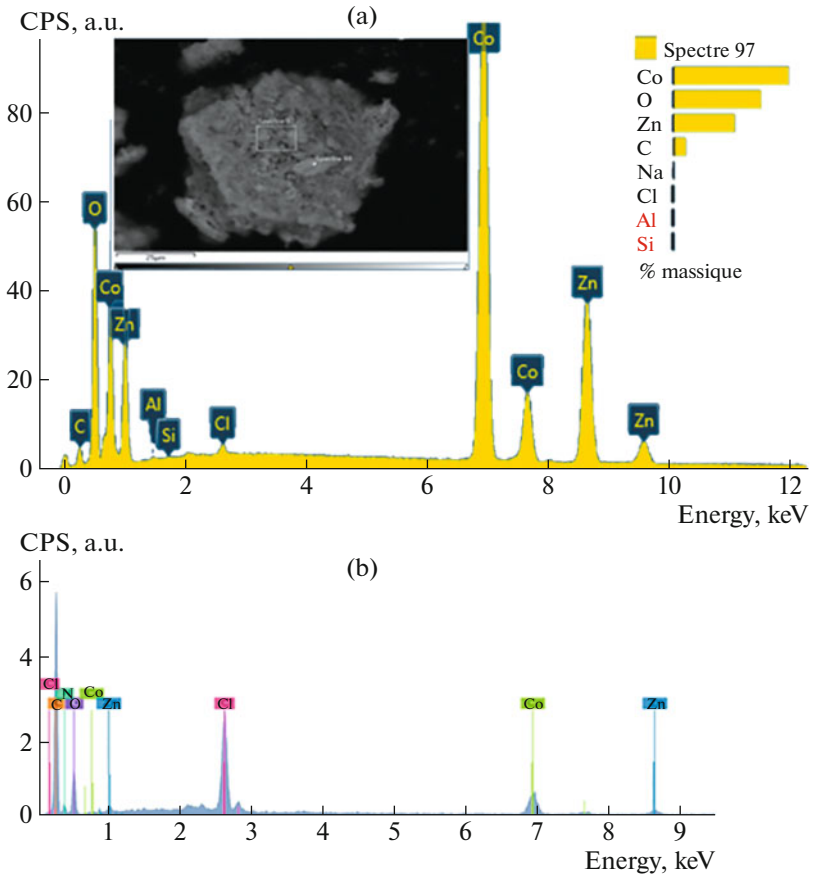

Fig. 4. EDX spectra of (a) $ZnCo_2O_4$ and (b) poly(Py-*co*-NMPy)-$ZnCo_2O_4$.

NMPy)-$ZnCo_2O_4$ hybrid material with a very high purity. The analysis also shows the presence of a quantity of chlorine (Cl) linked mainly to the precursor [41].

Solubility test represents the ability of the solvent to dissolve certain materials at a given temperature. It is shown that Ppy-$ZnCo_2O_4$ is insoluble in all the studied solvents, unlike to PNMPy-$ZnCo_2O_4$. The latter is well dispersed in chloroform, dichloromethane, THF, and *N*-methyl-2-pyrrolidone. Poly(Py-*co*-NMPy)-$ZnCo_2O_4$ is less soluble then PNMPy-$ZnCo_2O_4$.

CONCLUSIONS

The zinc cobaltite is synthesized by sol-gel method and is used to produce polypyrrole, poly(*N*-methyl pyrrole), and poly(pyrrole-*co*-*N*-methyl pyrrole) nanocomposites. The structure and morphology studies confirmed the production of the desired products.

FUNDING

This work is funding by La Direction Générale de la Recherche Scientifique et du Développement Technologique (DGRSDT) Algeria.

CONFLICT OF INTEREST

The authors declare that they have no conflict of interest.

REFERENCES

1. V. P. Ananikov, Nanomaterials **9**, 1197 (2019).
2. R. Mobin, T. A. Rangreez, H. T. N. Chisti, Inamuddin, and M. Rezakazemi, "Organic-Inorganic Hybrid Materials and Their Applications," in *Functional Polymers. Polymers and Polymeric Composites: A Reference Series*, Ed. by M. Jafar Mazumder, H. Sheardown, and A. Al-Ahmed (Springer, Switzerland, 2019).
3. S. L. Lee, and C.-J. Chang, Polymers (Basel, Switz.) **10**, 206 (2019).
4. J. Zou, H. L. Yip, S. K. Hau, and A. K. Y. Jen, J. Appl. Phys. Lett. **96**, 203301 (2010).
5. B. Z. Yang, Y. S. Lin, and J. M. Wu, Appl. Mater. Today **9**, 96 (2017).
6. M. Bharti, A. Singh, S. Samanta, and D. K. Aswal, Prog. Mater. Sci. **93**, 270 (2018).
7. R. B. Yang, P. M. Reddy, C. J. Chang, P. A. Chen, J. K. Chen, and C. C. Chang, Chem. Eng. J. **285**, 497 (2016).
8. H. Kang, H. Park, Y. Park, M. Jung, B. C. Kim, G. Wallace, and G. Cho, Sci. Rep. **4**, 5387 (2014).

9. C. J. Chang, M. H. Tsai, Y. H. Hsu, and C. S. Tuan, Thin Solid Films **516**, 5523 (2008).

10. M. Ates, M. El-Kady, and R. B. Kaner, Nanotechnology **29**, 175402 (2018).

11. C. J. Chang, Y. Y. Leong, C. F. Lai, W. Y. Chiou, M. J. Su, and S. J. Chang, J. Appl. Polym. Sci. **134**, 45210 (2017).

12. C. J. Chang, C. F. Lai, P. Madhusudhana Reddy, Y. L. Chen, W. Y. Chiou, and S. J. Chang, J. Lumin. **160**, 145 (2015).

13. T. Selvan, J. P. Spatz, H.-A. Klok, and M. Möller, Adv. Mater. **10**, 132 (1998).

14. T. Chena, Y. Fan, G. Wang, Q. Yang, and R. Yang, RSC Adv. **5**, 74523 (2015).

15. J. P. Morán-Lázaro, F. López-Urías, E. Muñoz-Sandoval, O. Blanco-Alonso, M. Sanchez-Tizapa, A. Carreon-Alvarez, H. Guillén-Bonilla, M. de la Luz Olvera-Amador, A. Guillén-Bonilla, and V. M. Rodríguez-Betancourtt, in *Nanostructured Materials—Fabrication to Applications,* Ed. by M. Seehra (IntechOpen, Rijeka, 2017), Chap. 8.

16. H. Liu, X.Wang, H. Xu, J. Wang, Q. Ma, W. Yu, Y. Yang, X. Dong, G. Liu, and Y. Zhao, RSC Adv. **8**, 39377 (2018).

17. N. Joshi, L. F. da Silva, H. Jadhav, J.-C. M'Peko, B. B. M. Torres, K. Aguir, V. R. Mastelaro, and O. N. Oliveira, Jr., RSC Adv. **6**, 92655 (2016).

18. Y. Sharma, N. Sharma, G. V. Subba-Rao, and B. V. R. Chowdari, Adv. Funct. Mater. **17**, 2855 (2007).

19. L. Huang, G. H. Waller, Y. Ding, D. Chen, D. Ding, P. Xi, Z. L. Wang, and M. Liu, Nano Energy **11**, 64 (2015).

20. C. Wu, J. Cai, Q. Zhang, X. Zhou, Y. Zhu, L. Li, P. Shen, and K. Zhang, Electrochim. Acta **169**, 202 (2015).

21. W. Fu, X. Li, C. Zhao, Y. Liu, P. Zhang, J. Zhou, X. Pan, and E. Xie, Mater. Lett. **149**, 1 (2015).

22. N. Joshi, L. F. da Silva, H. S. Jadhav, F. M. Shimizu, P. H. Suman, J.-C. M'Peko, M. O. Orlandi, J. G. Seo, V. R. Mastelaro, and O. N. Oliveira, Jr., Sens. Actuators, B **257**, 906 (2018).

23. M. Sharma and A. Gaur, Sci. Rep. **10**, 2035 (2020).

24. X. Wei, D. Chen, and W. Tang, Mater. Chem. Phys. **103**, 54 (2007).

25. F. Z. Kouidri, R. Berenguer, A. Benyoucef, and E. Morallon, J. Mol. Struct. **1188**, 121 (2019).

26. S. Senthilkumar and A. Rajendran, MOJ Polym. Sci. **1**, 192 (2017).

27. Q. Wang, L. Zhu, L. Sun, Y. Liub, and L. Jiao, J. Mater. Chem. A **10**, 1039 (2014).

28. A. O. Bokuniaeva and A. S. Vorokhm, J. Phys.: Conf. Ser. **1410**, 012057 (2019).

29. N. M. Juibari and A. Eslami, J. Therm. Anal. Calorim. **130** (2), 1 (2017).

30. M. Baskey, R. Maiti, S K. Saha, and D. Chakravorty, J. Appl. Phys. **115**, 094306 (2014).

31. M. Šetka, J. Drbohlavová, and J. Hubálek, Sensors **17**, 562 (2017).

32. B. Duran and G. zen Bereket, Ind. Eng. Chem. Res. **51**, 5246 (2012).

33. S. Bahraeian, K. Abron, F. Pourjafarian, and R. A. Majid, Adv. Mater. Res. **795**, 707 (2013).

34. S. Khademi, B. Pourabbas, and K. Foroutani, Polym. Bull. **75**, 4291 (2018).

35. A. Batoola, F. Kanwalb, M. Imranb, T. Jamilc, and S. A. Siddiqi, Synt. Met. **161**, 2753 (2012).

36. N. H. Bouabida, A. Hachemaoui, A. Yahiaoui, H. Gherras, A. Belfedal, A. Dehbi, and A.-H. I. Mourad, Polym. Sci., Ser. B **62**, 163 (2020).

37. A. Dehbi, A. H. I. Mourad, K. Djakhdane, and A. Hilal-Alnaqbi, Polym. Eng. Sci. **55**, 287 (2015).

38. K. Djakhdane, A. Dehbi, A. H. I. Mourad, A. Zaoui, and P. Picuno, Plast. Rubber Compos. **45**, 346 (2016).

39. H. Gherrass, A. Hachemaoui, A. Yahiaoui, A. Belfadel, A. Dehbi, and A. H. I. Mourad, J. Semicond. **39**, 102001 (2018).

40. I. Tiffour, A. Dehbi, A.-H.-I. Mourad, and A. Belfedal, Mater. Chem. Phys. **178**, 49 (2016).

41. Sachin. V. Bangale, S. M. Khetre, and S. R. Bamane, Chem. Sin. **2**, 303 (2011).

42. Y. Al Haj, J. Balamurugan, N. H. Kim, and J. H. Lee, J. Mater. Chem. A **7**, 3941 (2019).

43. A. Banerjee and Z. Singh, J. Solid State Electrochem. **13**, 1201 (2009).

44. H. J. Kim, I. C. Song, J. H. Sim, H. Kim, D. Kim, Y. E. Ihm, and W. K. Choo, Solid State Commun. **129**, 627 (2004).

45. C. R. Mariappan, R. Kumar, and G. Vijaya Prakash, RSC Adv. **5**, 26843 (2015).

46. D. O. Scanlon and G. W. Watson, Phys. Chem. Chem. Phys. **13**, 9667 (2011).

47. Y. Zhu, X. Ji, Z. Wu, W. Song, H. Hou, Z. Wu, X. He, Q. Chen, and C. E. Banks, J. Power Sources **267**, 888 (2014).

48. L. Hu, L. Wu, M. Liao, X. Hu, and X. Fang, Adv. Funct. Mater. **22**, 998 (2012).